

# Light Metals 2012

**ALUMINIUM PROCESSING**

*ORGANIZERS*

**Kai Karhausen**

Hydro Aluminium Rolled Products GmbH  
Bonn, Germany

**Edward Williams**

Alcoa  
Pittsburgh, Pennsylvania, USA

# Light Metals 2012

**ALUMINIUM PROCESSING**

## **Rolling**

*SESSION CHAIR*

**Kai Karhausen**

Hydro Aluminium Rolled Products GmbH

Bonn, Germany

## COMPARISON OF THE MICROSTRUCTURE AND TEXTURE EVOLUTION IN AA1050 ALUMINUM ALLOY SHEETS PRODUCED BY THE DC AND CC METHODS

Heber Pires Otomar<sup>1</sup>, Ronald Lesley Plaut<sup>2</sup>

<sup>1</sup>Eng., Msc. R&D Dept. of Votorantim Metals – CBA - Alumínio – SP – Brazil – heber.otomar@vmetaiscba.com.br;

<sup>2</sup>Assoc.Professor, Ph.D. – University of São Paulo- EPUSP/PMT – SÃO PAULO – SP - Brazil – rlplaut@usp.br

Keywords: Aluminum Alloys, Mechanical Working, Heat Treatment, Texture

### Abstract

This study aims to compare, on an industrial scale, of the effect of the direct chill (DC) and continuous casting (CC) fabrication processes of AA1050 rolled and annealed sheets. Characterization of their microstructure and texture evolution from the as-cast condition up to the end condition of a deep-drawn cup was carried out. Stamping tests were performed to identify which process presents best performance. Different microstructures were obtained for the studies processes: the DC material was more homogeneous, both in terms of intermetallic distribution and grain size. The mechanical properties of the CC material were slightly higher than those for the DC material. Forming Limit Diagram (FLD) of the homogenized CC material presented the best results.

### Introduction

This work aims to characterize the aluminum alloy AA1050 using different manufacturing processes and to identify their influence on the final sheet performance, employing tests that show how adequate the material is for forming operations. Briefly, the main objectives are:

- To evaluate influences of the manufacturing processes (CC x DC) of annealed sheets and coils (1.80mm of thickness) on their drawability.
- To characterize the microstructure and texture evolution throughout the manufacturing processes.

*Effect of casting process.* The continuous casting system (CC) is based upon the production of aluminum sheets from the passage of liquid metal through two water-cooled rolls. The plate thickness may vary from 2 to 12mm and the width from 750 to 2100mm, according to machine capacity.

For the sheet forming, the liquid aluminum is conducted through channels into the so-called injector, which distributes the metal throughout the width of the rolls. Once in contact with the cooled rolls, the aluminum solidifies at a cooling rate of around 300 - 700°C/s, much higher than that observed for the processing of plates. For highly alloyed alloys, the chemical elements tend to form supersaturated solid solutions.

For high cooling rates, intermetallic segregations are formed in the plate centerline, by dendrite formation, during the solidification process. This microsegregation can be harmful to the subsequent rolling processes since they can only be spread out through long homogenizing treatments.

*Effect of Texture in Aluminum Sheets.* The most frequent deformation texture components observed in aluminum and its alloys shows a predominance of the {112} <111> (type cooper texture), and {110} <112> (type brass texture) components, and sometimes the presence of the {011}<100> (type Goss type texture) and {123} <634> (S type texture) components (HÖLSCHER et al; 1994).

Changes in processing impose different textures and effects on subsequent forming processes. SARTORI (2002) has shown that recrystallized aluminum alloy AA1200, coming from the same

raw material, presented quite different effects, influenced by the material texture. This texture, resulting from the different processing stages, showed the unwanted effect of the cube {100} <011> texture component, presenting a larger degree of earing compared to samples which did not have predominantly this type of component. Further, this work showed that substantial gains could be obtained through the reduction of material losses, with earing reduction in the formed parts, as being one of the major benefits of the prior knowledge of the materials texture.

BENUM et al. (1994) found different textures associated with lubrication systems and/or rolling speeds, the shear texture components disappearing after increasing rolling speeds.

In many cases, texture determines the viability of using a given raw material in order to fulfill the forming requirements for a given application. From the study carried out by LIU and MORRIS, (2004), it is known that hot rolled plates have better forming performance when compared to materials produced from the caster type. However, it became apparent that texture was one of the components that justified such a difference.

*Effect on the Forming Limited Diagram (FLD).* The FLD is a diagram [major ( $\epsilon_1$ ) x minor strains ( $\epsilon_2$ )] that presents the plastic strain that a metallic sheet can withstand prior to the occurrence of a localized thickness reduction (upper limit) or formation of wrinkles (lower limit). It is regarded as being a subject of great importance in the sheet forming field. On the basis of experimental measurements, the concept of FLD was initially introduced by KEELER (1965) for the positive values of the minor ( $\epsilon_2$ ) strain measured in the plane of the sheet. This concept was then extended by GOODWIN (1968) and WOODTHORPE et al (1969) to the domain of negative strains.

It has to be pointed out that the path of different stress states are linear strain trajectories that remain constant during the process of deformation, yet at their end become closer to the plain strain condition. By joining these limiting points on the major/minor strain diagram, a FLD curve could be obtained, Richter (2003). In industry, it is common (yet very debatable), to consider that the strain limits do not depend on the type of test employed for their evaluation and represent, therefore, an “intrinsic” property of the material.

### Materials and Methods

The target of this work is to conduct a comparative analysis between sheets of an AA 1050 aluminum alloy, cold-rolled and annealed, that were obtained through two distinctive solidification processes. The selected processes were those locally available ones (with largest usage) by customers of CBA, which produce stampings, mainly domestic utensils, such as pans and casseroles. For the sake of a more complete analysis, a third sheet processing route was included in this study, namely starting from CC, with an intermediate homogenization (after 35.7% cold rolling). Table I presents the analyzed conditions and the nomenclature given to the samples and processes/routes.

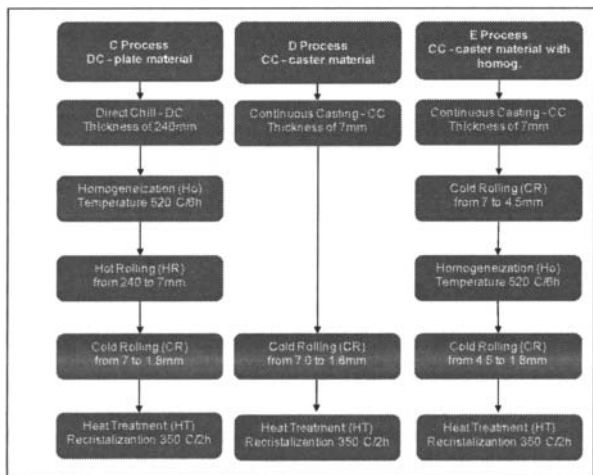


Figure 1 - Flowchart of manufacturing processes for the AA1050 alloy

Due to the advantages of the CC method, mainly in relation to the reduction in the number of processing stages (as shown in figure 1), the focus of the analysis will be by starting from the stage where the plates had the same thickness, i.e. prior to cold rolling, this being the starting point for the comparative analysis.

Chemical composition was evaluated using optical emission spectroscopy (ARL-model3460) on previously sand papered samples.

Optical Microscopy was performed on the samples taken at the surface,  $\frac{3}{4}$  and  $\frac{1}{2}$  thicknesses. Samples were prepared using sandpaper and final polishing with diamond paste (3 microns). Precipitates were revealed using HF 0.5% in water. Grain structure was obtained through anodic oxidation in Baker solution. All images were obtained with an Olympus BX51M optical microscope. For the macrotexture, samples were prepared following the same procedure as for the optical microscopy until the polishing stage. An automatic texture goniometer (with 5° steps, connected to a Rigaku -mod. DMAX-2000 diffractometer-from IPEN, employing MoK $\alpha$ 1 radiation  $\lambda=0,7093\text{\AA}$ ), was used. Ultimate Tensile Strength (UTS), Yield Strength (YS) and Elongation have been evaluated in accordance with ASTM 515-5 using a tensile machine (EMIC- mod. DL 5000).

Earing tests were carried out on an Erichsen- mod. 145-60 machine. The FLD curve was evaluated from tests performed in the Mechanical Testing Lab. of CBA, using the criteria established by the ASTM E 2218-02 - "Standard Test for Determining Forming Limit Curves". It defines the testing parameters, grating circle dimensions and the numbers of samples (in this case, three samples for each sample dimension).

## Results and Discussions

Table 1 summarizes the different conditions that have been studied.

### Optical Microscopy (OM).

Figure 2 presents the granular structure of the as-cast DC – plate material, where it may be observed that in the sample centre (figure 2b), the grain size is smaller than at the periphery. The structure presents the "Chinese script", probably  $\alpha$ -phase (AlFeSi), formed between the dendrite arms during solidification (BACKERUD, KRÓL and TAMMINEM; 1968). This structure is

typical of a relatively low solidification rate, of the order of 1 to 5°C/s, characteristic of the DC process.

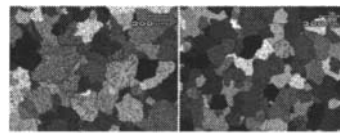


Figure 2 – OM of the microstructure of the DC – plate material (C0) as-cast conditions (polarized light), in the longitudinal section being: a) surface; b) center of thickness

Table I - Identification of the samples as a function of the process and condition of the material.

| Alloy / Type                      | Sample Ident. | Stage of the process / Condition of the sample    |
|-----------------------------------|---------------|---|
| DC - Plate Material               | C0            | As-cast thickness of 240 mm                       |
|                                   | C1            | After HR / Rolling 7mm                            |
|                                   | C2            | After CR / Work hardening in thickness from 1.8mm |
| CC - Caster Material              | D1            | As-cast thickness of 7 mm                         |
|                                   | D2            | After CR / Work hardening in thickness from 1.8mm |
|                                   | D3            | After HT / Annealed in thickness from 1.8mm       |
| CC - Caster Material (Interm. Ho) | E1            | As-cast thickness of 7 mm                         |
|                                   | E2            | After CR / Work hardening in thickness from 4.5mm |
|                                   | E3            | After HT / Homogenized in 4.5 thick               |
|                                   | E4            | After CR / Work hardening in thickness from 1.8mm |
|                                   | E5            | After HT / Annealed in thickness from 1.8mm       |

HR - Hot Rolling / CR - Cold Rolling / HT - Heat Treatment

The material of the DC process (figure 3a) presents a partially recrystallized grain structure, with irregular morphology, which is typical to the hot rolling condition. In the plate center, a more deformed structure can be observed as compared to the one on the surface. This condition can be associated with Fe-segregation that may inhibit recrystallization during hot rolling.

The material coming from the CC caster process presented a deformed structure due to hot forming of the material straight after the solidification started between the rolls. At the surface, the grains have an orientation of approximately 45° in relation to the solidification direction this value, reducing as we move to the sample centerline (figure 3b).

### Materials in the as-cast condition

CC – caster material (D3, E5) presented a central region with a segregated structure with intermetallics, figures 4c, 4d and 5.

CC – caster material (D3) the intermetallics are more finely distributed than CC-Caster process (E5), with an intermediate homogenization (figure 5), that presented a structure of coarser precipitates, still in this process, the intermetallics on the surface are smaller than at the center (figure 5).

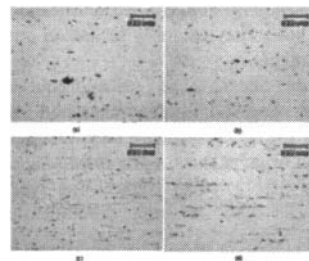


Figure 4 - Micrograph in the longitudinal section of metal, DC – plate material (C3 sample); a) surface; b) center; CC – caster material (D3sample); c) surface; d) center of thickness.

DC – plate material (C3) presented a matrix with a smaller amount of precipitates, having a volumetric fraction of 1.20% against 1.30% for the sample E5 and 2.10% for the D3 sample.

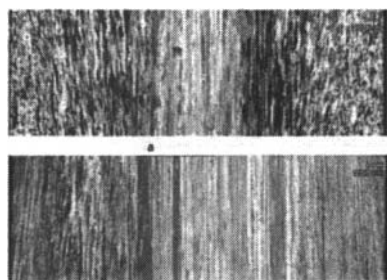


Figure 3- Microstructure before cold rolling (OM-polarized light) were  
a) DC – plate material (C1) hot rolled to 7.0mm;  
b) CC – caster material (D1) as-cast with 7.0mm

*Material in the final HR-condition.*

DC – plate material (C3) presented a structure with a grain size of around 32µm, figure 6a, 6b.

CC - caster material (D3) presented a grain size of 52µm however heterogeneous and larger in the surface than in the center (figure 6c and 6d).

CC – caster material with an intermediate homogenization (E5) presented an average grain size of 40µm, more homogeneous (figure 7) than CC – caster material without the homogenization (D3), however.

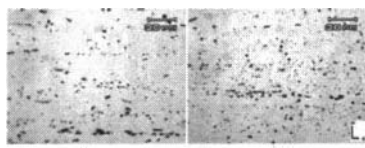


Figure 5 - Micrograph in the longitudinal section CC-caster material with homog. (E5) were; a) surface, b) center of thickness.

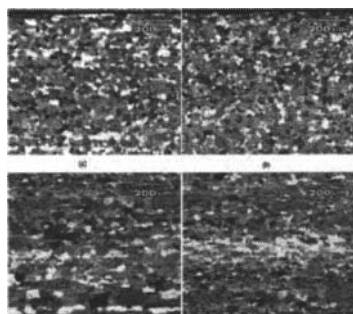


Figure 6 - Microstructure of the longitudinal section after cold rolling and annealing were;  
a) surface of DC – plate material (C3),  
b) center of DC – plate material (C3),  
c) surface of CC – caster material (D3) and  
d) center of CC – caster material (D3)

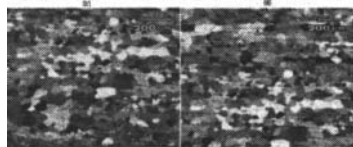


Figure 7 - Microstructure of the longitudinal section after cold rolling and annealing CC – caster material with homog. (E5);  
a) surface, b) center of thickness

The graph in figure 8 demonstrates the variation of grain size throughout the thickness of the material. It is possible to observe the increase in the grain size towards the CC – caster materials (D3 and E5), and a smaller grain size towards the surface.

DC – plate material presents a homogeneous distribution. This difference is related to the solidification rate; in the CC – caster

materials this rate is very high, hence propitiates greater intermetallic segregation, affecting recrystallization kinetics and hence grain growth. In the CC – caster material with an intermediate homogenization (E5 sample) this trend also prevails.

Table II - Parameters of cold rolling

| Sample         | Thickness  |             | Reduction | Work roll     |     |
|----------------|------------|-------------|-----------|---------------|-----|
|                | input (mm) | output (mm) |           | diameter (mm) | l/h |
| C – 1050 DC    | 7,0        | 4,0         | 43%       | 398           | 3.5 |
|                | 4,0        | 2,4         | 40%       | 398           | 4.5 |
|                | 2,4        | 1,8         | 25%       | 348           | 4.3 |
| D – 1050 CC    | 7,0        | 4,0         | 43%       | 398           | 3.5 |
|                | 4,0        | 2,4         | 40%       | 398           | 4.5 |
|                | 2,4        | 1,8         | 25%       | 348           | 4.3 |
| E – 1050 CC ho | 7,0        | 4,5         | 36%       | 398           | 3.2 |
|                | 4,5        | 2,4         | 47%       | 398           | 4.5 |
|                | 2,4        | 1,8         | 25%       | 348           | 4.3 |

*Tensile test and Hardness measurements.* Tensile testing was carried out on the samples taken in three distinct stages, namely; at the start of rolling (where the samples had a thickness of 7.0mm); with 1.80mm thickness (after cold rolling), both in the work-hardened state and after the annealing heat treatment.

The results are summarized in table III, from which it is possible to observe the following aspects:

a) At the beginning of processing, the materials proceeding from CC - caster, presented higher UTS and YS values as compared to the materials coming from the DC-plate route, as can be seen from samples C1, D1 and E1. This condition is explained by the small deformation that occurs in the caster process, being about 15%, causing hardening and consequent increase in hardness. (WESTENGEN, 2000; TRICIBAR, 1999)

b) After cold rolling, mechanical properties showed some differences. The CC – caster material that presented a major increase in UTS (D2) due to work hardening (74%) to the CC – caster material with an intermediate homogenization (E4) that was less work hardened (60%).

Comparing these results with the available information given, for instance on the *AluMatter* site (table III), it is possible to evaluate that the hardness expected for this alloy (after cold rolling and annealing) is 21HB, a value which has not been reached for any of the studied materials. For these, the average values obtained were higher than 42HB, without significant variations between samples.

The YS, which basically could be taken as an indication of formability (Dieter, Bacon; 1988), also presented higher than expected values. However, in this case, the CC-caster material, without homogenization, stayed at a highest level, presenting a YS of 48MPa (sample D3), against 40MPa for the CC-caster material with intermediate homogenization (sample E5).

Confirming the values provided by the *AluMatter* site (<http://www.aluminium.matter.org.uk>), ZHOU et al. (2003) identified that, with an annealing treatment, the YS values fell within the range of 35 to 40MPa.

*Texture After Cold Rolling.* Texture analysis was performed on samples taken after cold rolling(74% reduction) for the DC and CC materials without homogenization (samples C3 and D3) and 60% for the CC homogenized material (sample E5). Under these conditions, the {001} <110> rotated cube component becomes more intense for cold reductions larger than 60% (LIU and MORRIS, 2003).

The DC material started cold rolling with a predominance of the rotated cube and Goss type textures. After the cold working, the predominant texture observed was the Dillamore type  $\{4\ 4\ 11\}\langle 11\ 11\ \bar{8}\rangle$  and one of its variants  $\{11\ 11\ 8\}\langle 4\ 4\ \bar{1}\bar{1}\rangle$  (Figure 9). The  $S\sim\{123\}\langle 634\rangle$  texture component was also identified.

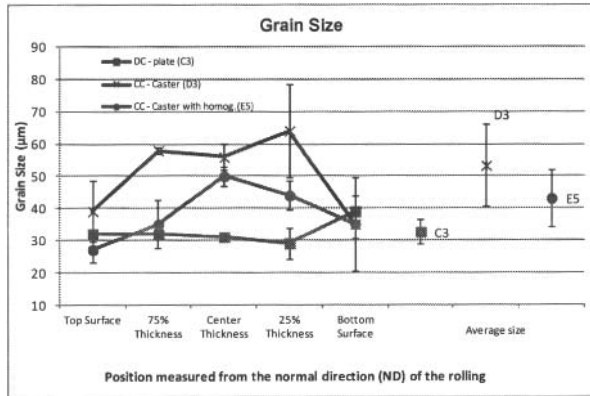


Figure 8 - Comparative graph of the grain size along the thickness after annealing for 1h by 350°C

The emergence of this  $\{11\ 11\ 8\}\langle 4\ 4\ \bar{1}\bar{1}\rangle$  component may be associated with the rolling conditions, such as temperature, lubrication and, in some cases, due to inhomogeneous deformation, i.e., the ratio between the radius of the rolls and the average thicknesses (between entry and exit thickness) on the mill. This ratio is given by  $l/h$  ( $l$  = contact arc and  $h$  = average thickness). This ratio should be ideally situated between 0.5 and 5.0., higher values causing shear stresses on the sheet surface (MISHIN et al; 2000). According to table II, the  $l/h$  ratio is within the suggested range; the two last rolling passes had values closer to the maximum of the  $l/h$  ratio (4.5), suggesting that this could also be an influencing factor on the differences between the material textures. As mentioned before, the rolling parameters (speed and/or lubrication) should also affect the emergence of that texture (BENUM et al; 1994).

Figure 10 presents the texture evolution for all studied processes. It is possible to see the variations of intensity along the process steps.

Table III –Mechanical properties of studied samples compared to the typical properties (1) for the AA1050 alloy.

| Description   | UTS (MPa) | YS (MPa) | Elongation (%) | Hardness (HB) |
|---|-----------|----------|----------------|---------------|
| C1 - Hot Rolling  | 80        | 54       | 47             | 27            |
| D1 / E1 - As-cast   | 108       | 87       | 32             | 38            |
| C2 - Hardening of 75%   | 153       | 141      | 7              | 39            |
| D2 - Hardening of 74%   | 170       | 160      | 6              | 48            |
| E4 - Hardening of 60%   | 138       | 131      | 12             | 44            |
| C3 - Work hardening and annealed with 1.80mm                  | 74        | 42       | 43             | 41            |
| D3 - Work hardening and annealed with 1.80mm                  | 74        | 48       | 45             | 42            |
| E5 - homogenized, work hardening and annealed with 1.80mm     | 80        | 40       | 46             | 42            |
| Typical Values of the alloy AA1050 - Annealed "O" (1)         | 80        | 35       | nd             | 21            |
| Typical Values of the alloy AA1050 - Work hardening "H18" (1) | 180       | 170      | nd             | 48            |

*Texture in samples after cold rolling and subsequent annealing.* Under final conditions, i.e., after cold rolling and annealing at 350° C for 2h, the materials presented, in general, a more pronounced Goss  $\{011\}\langle 100\rangle$  type texture and recrystallization and rolling components (see figures 13, 14 and 15).

The DC- plate material (C3) presented the Goss component, as shown in figures 10 and 13. At the surface of this material, it is

possible to identify the Dillamore  $\{4\ 4\ 11\}\langle 11\ 11\ \bar{8}\rangle$  component, which is typically a shear component, as previously mentioned, presenting an intensity of  $f(g) = 4.60$ , smaller only than the Goss component, which presented  $f(g) = 7.30$ , (see figure 13).

The CC- caster material (D3) has a more intense Goss texture at the surface if compared with the center, with values of  $f(g) = 7.50$  and 6.10, respectively (figure 15). Also the texture components, identified as being  $\{115\}\langle 555\rangle$ , has an intensity of  $f(g) = 3.60$  at the surface against 4.50 at the center.

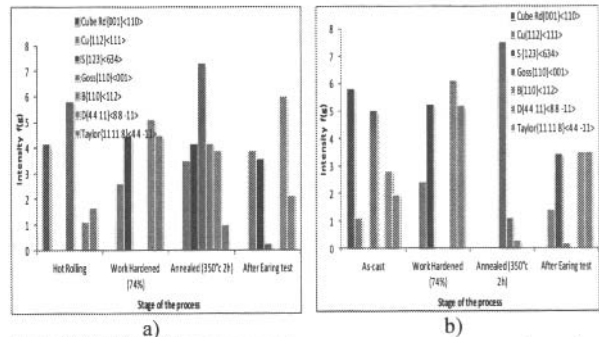
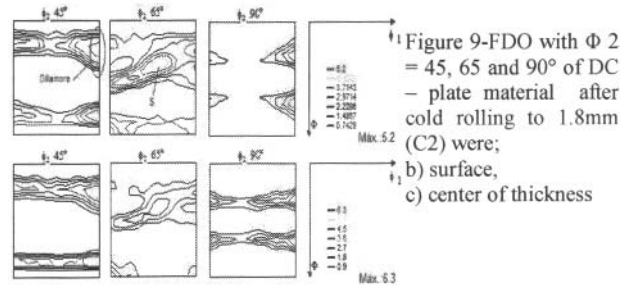


Figure 10 – Texture intensity variation in the surface of the samples during the manufacturing stages, a) route "C" - DC plate; b) route "D" - CC caster; c) route "E" - CC caster with intermediate homogenization.

The CC-caster material with an intermediate homogenization (E5) presented at the surface a larger intensity of the  $\{115\}\langle 555\rangle$  texture component, with  $f(g) = 4.50$ . The Dillamore texture component (with a lower intensity,  $f(g) = 2.90$ ) and the cube type texture (with a lower intensity,  $f(g) = 1.30$ ) were also identified. In the intermediate region (about 75% thickness), the textures did not show significant changes (figure 14b). At the sample centre, the Goss type texture (that was not identified at the surface), presented the greatest intensity, with  $f(g) = 5.60$ , against 4.50 for the Dillamore component and 3.80 for the  $\{115\}\langle 555\rangle$  texture component (figure 14c). The Cube texture practically does not appear, this condition being associated with the recrystallization temperature used in this process, where the kinetics of recrystallization was high enough to make the

emergence of this component unlikely; such situations have been studied by SAETER and NES (1998).

Table IV – Earing test results

| Sample                        | Index of medium | Number and direction  |
|-------------------------------|-----------------|-----------------------|
|                               | ear             | of the ear            |
| C3 - Alloy AA1050-O / DC      | 4.06%           | 4 ears (0/90°)        |
| D3 - Alloy AA1050-O / CC      | 1.84%           | 8 ears (0/45/90/135°) |
| E5 - Alloy AA1050-O / CC - ho | 4.02%           | 4 ears (45/135°)      |

*Texture after the earing test.* For the purpose of characterization of rolled and annealed samples, texture evolution after earing test was also evaluated; see table IV. This test simulates forming conditions, revealing the influence of the texture on the earing appearance in cups (figure 16). In figure 10a, the DC – plate material (C3) shows an increase in the intensity of the Dillamore component from  $f(g) = 3.9$  to  $6.0$  ~ after the earing testing. The CC- caster material did not exhibit major modifications after cup forming (figure 10b), keeping roughly the same texture components and intensities. Only the material with intermediate homogenization maintained the Goss component at  $f(g) = 7.5$  at the surface (figure 10c).

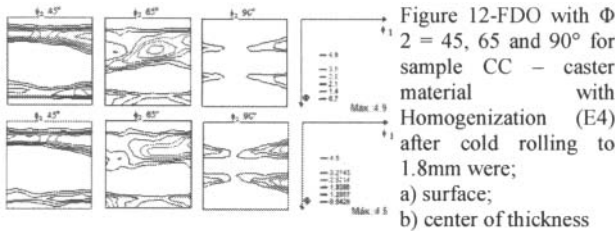


Figure 12-FDO with  $\Phi 2 = 45, 65$  and  $90^\circ$  for sample CC – caster material with Homogenization (E4) after cold rolling to 1.8mm were; a) surface; b) center of thickness

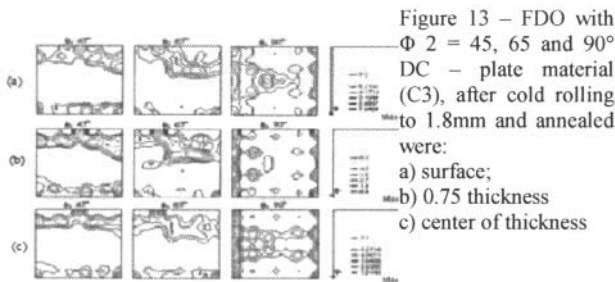


Figure 13 – FDO with  $\Phi 2 = 45, 65$  and  $90^\circ$  DC – plate material (C3), after cold rolling to 1.8mm and annealed were: a) surface; b) 0.75 thickness c) center of thickness

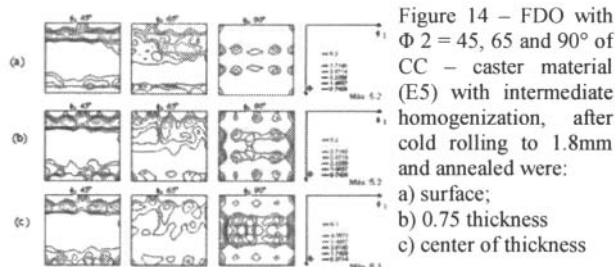


Figure 14 – FDO with  $\Phi 2 = 45, 65$  and  $90^\circ$  of CC – caster material (E5) with intermediate homogenization, after cold rolling to 1.8mm and annealed were: a) surface; b) 0.75 thickness c) center of thickness

*Forming Limit diagram (FLD).* The FLD obtained for the studied materials is presented in Figure 17. From this curve, it is possible to conclude that the intermediate homogenization performed on the CC-caster significantly improved formability of the material,

since the FLD presented an increase of ~25% for the plain strain region (or rather, for a of strain  $\epsilon_2 = 0$ ).

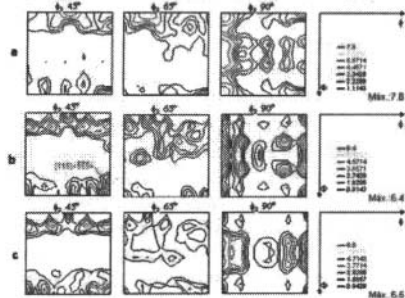


Figure 15 – FDO with  $\Phi 2 = 45, 65$  and  $90^\circ$ , CC – caster material (D3) after cold rolling to 1.8mm and annealed were: a) surface; b) 0.75 thickness c) center of thickness



Figure 16 – schematic drawing of the sample taken for texture analysis, following the earing test.

It may be also observed that the DC-plate material (C1) presented an intermediate condition between the CC- caster processes. In Figure 17, the curve obtained by KOHARA (1993) was also included, in order to compare results. It may be observed that there is good agreement with present results. On the left side of the curve, (which is the region related to deep drawing), the CC-caster material without homogenization (D3) presented the lowest curve as compared to the other conditions, including the results from literature. The other material conditions (C3 and E5) showed similar results and, again, very close to ones from the literature, indicating that for these strain states, material performance should be similar.

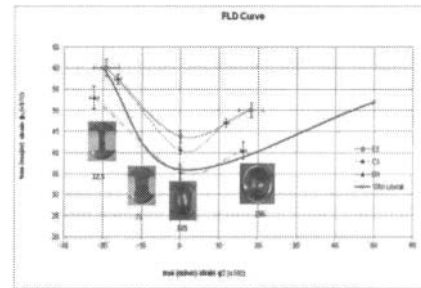


Figure 17 – FLD obtained for the samples studied, compared with the curve from the literature - Kohara (1993).

### Conclusions

Conclusions will be addressed to in accordance with the steps performed in this analysis.

*Metallographic structure.* The microstructures of the materials studied followed the expected trend and in-depth studies by other research, both the for DC and CC production processes. These showed that for the CC-caster, there is a microstructure containing intermetallic areas segregating the center from the surface, while the DC - plate material does not present this condition. Grain structure presented similar characteristics between the processes studied; however, the CC-caster material presented greater heterogeneity. The CC-caster material with an intermediate homogenization process resulted in a microstructure with larger grain size than the material with no homogenization; however there was less heterogeneity when compared to the CC-caster material without intermediate homogenization.

**Texture.** Texture evolution presented characteristics of  $\{001\}\langle 110 \rangle$  rotated cube type at the beginning of the process (in the hot rolled plate and in the CC-caster in the as- solidified state) It was more pronounced for the material produced from the CC-caster than from the DC- plate. After cold rolling, all the studied processes/routes showed a Dillamore type component  $\{4\ 4\ 11\}\langle 11\ 11\ \bar{8} \rangle$  (typically associated with shear stress). The CC-caster material processed with homogenization presented a lower intensity of this component relative to other processed materials. This condition may be related to the different strain level before annealing. In the final condition (cold rolled and annealed), all materials presented the  $\{1\ 0\ 0\}\langle 0\ 1\ 1 \rangle$  Goss type component, with a greater intensity. However, the surface of the CC-caster material, with intermediate homogenization, did not show this texture component.

**Mechanical Properties.** The yield strength of all materials was higher than the reference value used to compare these materials with other studies, the reason being associated with chemical composition, mainly Fe and Si or the grain size obtained in this experiment. Intermediate homogenization produced materials with YS close to the DC-plate route. The CC-caster material without homogenization presented the largest YS value.

**Formability behavior.** The CC-caster, with intermediate material homogenizing, presented more favorable forming conditions than the other processed materials, including those of the DC-plate material as opposed to values mentioned in the references. This improvement might be associated with the intermediate homogenization treatment, as the material showed a 60% reduction against a 74% reduction given to the DC-plate and CC-caster processes/routes respectively prior to final annealing.

All processes presented an FLD within the expected limits for this alloy, indicating that the processes/routes that were adopted are not far from those normally used/studied.

#### Acknowledgements

The authors would like to thank the Votorantim Metals – CBA for supplying the material used in the present investigation and IPEN – Nuclear and Energy Research Institute that made the x-ray tests on the samples for the macrotexture.

#### References

- BACKERUD, L., KROL, E., Tamminen, J., Solidification Characteristics of Aluminium Alloys, Sweden, Skan Aluminium, p75-84, 1986.
- BENUM, S., ENGLER, O., NES, E., Rolling And Annealing Texture In Twin Roll Cast Comercial Purity Aluminium, Materials Science Forum Vols. 157-162, p913-918, 1994.
- DIETER, G. E., BACON, D., Mechanical Metallurgy, McGraw-Hill, 1988.
- GOODWIN, G. M., Application Of The Strain Analysis To Sheet Metal Forming In The Press Shop, La Metallurgia Italiana, v.8, p767-774, 1968.
- HÖLSCHER, M., RAABE, D., LÜCKE, K., Relationship Between Rolling Texture And Shear Texture in F.C.C. And B.C.C. Metals, Acta Metall. Mater Vol. 42 No.3, p879-886, 1994.
- KEELER, S. P., Determination Of The Forming Limits In Automotive Stamping, Sheet Metal Industries, v42, p683-691, 1965.
- KOHARA, S., Forming Limit Curves Of Aluminum And Aluminum Alloy Sheets And Effects Of Strain Path On The

Curves, Journal of Materials Processing Technology, v.38, p723-735, 1993.

LIU, J., MORRIS, J., G., Macro-,Micro-And Meso Texture Evolutions Of Continuous Cast And Direct Chill Cast AA3105 Aluminum Alloy During Cold Rolling, Materials and Engineering A357 p277-296, 2003.

LIU, J., MORRIS, J. G., Recrystallization microstructures and textures in AA 5052 Continuous Cast And Direct Cast Aluminum Alloy. Materials Science and Engineering, A385, p342-351, 2004.

MISHIN, O. V., BAY, B., JENSEN, D. J., Through-thickness texture gradients in cold-rolled aluminum, Metallurgical And Materials Transaction, v.13, p1653-1662, 2000..

RICHTER, A., Comparação dos resultados de diferentes testes para a determinação da curva limite de conformação, In: Conferência Nacional de Conformação de Chapas, 4, Porto Alegre, Porto Alegre (Brasil), p24-29, 2003.

SAETER, J.A., NES, E., Influence of Minor Precipitation Reactions on the Development of Recrystallisation Textures in Commercial Purity Aluminium, Materials Science Forum vols. 273-275, p477-482, 1998.

SARTORI, A., SANDIM, H. R. Z., Evolução Da Textura Tipo Cubo No Recozimento Final Da Liga AA1200 E Sua Influência Na Estampagem., In: Congresso Internacional de Tecnologia da Indústria do Alumínio. 1, São Paulo, 2002, São Paulo, ABAL, 2002. p664-675, 2002.

TRICIBAR, R., Jin, L., Rolling Aspects Of Twin Roll Casting, Light Metals, p1129-1143, 1999.

WESTENGEN, H., Twin roll casting of aluminium, Light Metals, p1111-1127, 2000.

WOODTHORPE, J., PEARCE, R., The effect of r and n upon the forming limit diagrams of sheet metal, Sheet Metal Industries, p1061-1067, 1969.

ZHOU, X.S., ZHONG, J., MAO, D., FUNKE, P., Experimental Study On Material Properties Of Hot Rolled And Continuously Cast Aluminum Strips In Cold Rolling, Journal of Materials Processing Technology, v.134, p352-362, 2003.